



HAL
open science

High content Super-Resolution Imaging of Live Cell by uPAINT.

Gregory Giannone, Eric Hosy, Jean-Baptiste Sibarita, Daniel Choquet,
Laurent Cognet

► **To cite this version:**

Gregory Giannone, Eric Hosy, Jean-Baptiste Sibarita, Daniel Choquet, Laurent Cognet. High content Super-Resolution Imaging of Live Cell by uPAINT.. *Methods in Molecular Biology*, 2013, 950, pp.95-110. 10.1007/978-1-62703-137-0_7 . hal-00796947

HAL Id: hal-00796947

<https://hal.science/hal-00796947>

Submitted on 5 Mar 2013

HAL is a multi-disciplinary open access archive for the deposit and dissemination of scientific research documents, whether they are published or not. The documents may come from teaching and research institutions in France or abroad, or from public or private research centers.

L'archive ouverte pluridisciplinaire **HAL**, est destinée au dépôt et à la diffusion de documents scientifiques de niveau recherche, publiés ou non, émanant des établissements d'enseignement et de recherche français ou étrangers, des laboratoires publics ou privés.

High-content super-resolution imaging of live cell by uPAINT

Grégory Giannone^{1,2}, Eric Hosy^{1,2}, Jean-Baptiste Sibarita^{1,2}, Daniel Choquet^{1,2}, Laurent Cognet^{3,4}

¹Univ. de Bordeaux, Interdisciplinary Institute for Neuroscience, UMR 5297, F-33000 Bordeaux,

²CNRS, IINS UMR 5297, Bordeaux, France

³Univ Bordeaux, LP2N, F-33405 Talence, France

⁴CNRS & Institut d'Optique, LP2N, F-33405 Talence, France

Summary/Abstract

In this chapter, we present the uPAINT method (Universal Point Accumulation Imaging in the Nanoscale Topography), a simple single-molecule super-resolution method which can be implemented on any wide field fluorescence microscope operating in oblique illumination. The key feature of uPAINT lies in recording high numbers of single molecules at the surface of a cell by constantly labeling while imaging. In addition to generating super-resolved images, uPAINT can provide dynamical information on a single live cell with large statistics revealing localization-specific diffusion properties of membrane biomolecules. Interestingly, any membrane biomolecule that can be labeled with a fluorescent ligand can be studied, making uPAINT an extremely versatile method.

Key Words

Super-resolution microscopy, single molecule detection, high-density single particle tracking, nanoscopy, membrane biomolecule dynamics

1. Introduction

By pushing optical resolutions down to the scale of the molecules themselves, super-resolution optical microscopy techniques have revolutionized biomolecular imaging in cells(1, 2). Super-resolved images obtained from single molecule detections are in fact the collection of the super-localizations of single emitters imaged successively at low density on the specimen of interest. This is usually performed by iteratively activating a small number of photo-activable fluorophores among a dense

population of inactivated ones. Such approaches inherently require photo-activable or photo-switchable fluorophores which can be either engineered fluorescent proteins (PALM(3, 4)) or dyes immersed in reducing agents to allow the photo-conversion (STORM(5)). Importantly, these methods have difficulties to access very densely labeled regions due to spontaneous photoswitching, which prevents imaging individual fluorophores in these regions (6). Furthermore, up to now, neither PALM nor STORM allow the versatile study of endogenous molecules at nanometer resolutions on live cells(2). For this purpose, the universal PAINt (uPAINt) method (7) which generalizes the Point Accumulation Imaging in the Nanoscale Topography was developed (8). uPAINt does not require the photoactivation of single molecules and it is instead based on the real time imaging and tracking of single fluorescent ligands while they label their membrane biomolecular targets (**Fig. 1**). In other words, the single emitters are imaged at low density upon labeling as opposed to other single molecule based super-resolution methods where the samples are labeled prior to imaging at high density and stochastic photoactivation is used during the imaging sequence.

One of the key features of uPAINt is to image in real time single fluorescent ligands binding to their target. For this purpose, high affinity luminescent ligands are placed in the recording medium at the appropriate concentration under the microscope so that single molecules can be imaged and their trajectories can be isolated. Oblique illumination is required in order to selectively excite fluorescent ligands that have bound to their target and not those present in solution above the cellular membrane. Akin to any single molecule based super-resolution method, image analysis is an important step. Furthermore, as thousands of long lasting trajectories can be obtained on single cells with uPAINt, the amount of information generated per cell is considerable. It thus requires adequate dynamic analysis and visualization strategies to be handled. The following sections will describe each of these steps and discuss the protocols in order to successfully achieve results from uPAINt experiments.

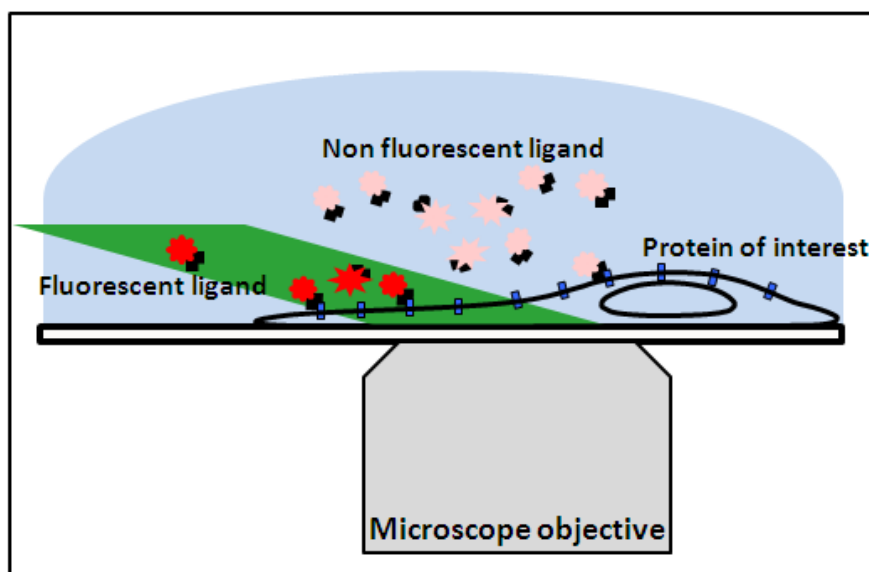


Figure 1: The Principle of uPAINT is based on the real-time imaging and tracking of single fluorescent ligands while they label their membrane biomolecules targets. A low concentration of fluorescent ligands is introduced in the extracellular medium such that a constant rate of membrane molecules is being labeled during the imaging sequence. Oblique illumination of the sample is used to excite predominantly fluorescent ligands, which have bind to the cell surface while not illuminating the molecules in the above solution

2. Materials

There are different types of equipment needed for successful uPAINT experiments. They are used for labeling, acquisition and image processing. Examples of equipment and their suppliers used in our laboratories are listed below.

2.1 Reagents:

1. Fluorescence free immersion oil (FF Cargille)
2. Fluorescent Tetraspec beads (Invitrogen) for image registration.
3. Protein labeling kit for obtaining fluorescent ligands e.g.: antibodies coupled to NHS ester Atto dyes (ATTO-TEC GmbH) or NHS ester Cy3/Cy5 dyes (Amersham CyDye™ Antibody Labeling Kits, GE Healthcare Life Sciences)
4. Salt based recording medium: 100 mM NaCl, 5 mM KCl, 10 mM Glucose, 2 mM CaCl₂, 2 mM MgCl₂, at pH=7.4 (Hepes 20 mM / NaOH).
5. Ringer medium: 150 mM NaCl, 5 mM KCl, 2 mM CaCl₂, 2 mM MgCl₂, 10 mM HEPES, 11 mM Glucose, at pH 7.4) (if performing exogenous labeling; see **Section 3.3, step 1**).
6. Trypsin/EDTA (if performing exogenous labeling)(Invitrogen, Gibco).
7. Phosphate Buffer Solution (PBS)(Euromedex)
8. Bovine Serum Albumin (BSA)(Sigma-Aldrich)
9. Dimethyl Sulfoxide (DMSO)(Sigma-Aldrich)
10. Gel filtration column filled with G-25 Sephadex (Sigma-Aldrich)
11. Dulbecco's Modified Eagle Medium (DMEM)(Invitrogen, Gibco)
12. Fetal Bovine Serum (FBS)(Invitrogen, Gibco)
13. Rat collagen I or human fibronectin (Roche)
14. Poly-lysine solution (Sigma-Aldrich)
15. Amaxa Nucleofactor II Device (Lonza)
16. Neurobasal Medium (Invitrogen, Gibco)

2.2 Instrumentation:

1. Inverted microscope (Olympus IX 71, Nikon TiE or equivalent)
2. High NA (1.45 or 1.49) oil immersion objectives
3. Continuous Wave (cw) lasers for excitation depending on the fluorophore to be imaged: E.g., 23mW HeNe laser (Thorlabs), frequency doubled Nd:Yag (Coherent) or solid state lasers.
4. Low noise highly sensitive electron multiplying CCD camera: E.g., QuantEM or Cascade (Photometrics)
5. Several optical and opto-mechanical components including mirror and lenses.
6. Fast shutter (Uniblitz) or AOTF (AA optoelectronic).
7. For each dye, an appropriate set of filters (Chroma or Semrock) is required
17. Fluorescence free immersion oil (FF Cargille)
8. Ludin opened sample holder (Life Imaging Services)
9. Microscope temperature (37°C) control system (Life Imaging Services)
18. Fluorescent Tetraspec beads (Invitrogen) for image registration.: 100 mM NaCl, 5 mM KCl, 10 mM Glucose, 2 mM CaCl₂, 2 mM MgCl₂, at pH=7.4 (Hepes 20 mM / NaOH). Ringer medium: 150 mM NaCl, 5 mM KCl, 2 mM CaCl₂, 2 mM MgCl₂, 10 mM HEPES, 11 mM Glucose, at pH 7.4) (if performing exogenous labeling; see **Section 3.3, step 1**). Trypsin/EDTA (if performing exogenous labeling). Fugene 6 (Roche) (if performing exogenous labeling)
10. Computer for image acquisition
11. Software for image acquisition (Metamorph)
12. Computer for image processing and visualization
13. Software for image processing and visualization (Metamorph, ImageJ, Matlab)

3. Methods

3.1 Optical setup

Image acquisition of single molecules with high signal-to-noise ratio is a critical step for efficient reconstruction of super-resolved images. The final nanometric resolution will directly depend on this signal-to-noise ratio(9, 10).

3.1.1 Microscope

This protocol was optimized using an inverted microscope equipped with a 1.45 NA 100X oil immersion objective. Highly fluorescent organic dyes (e.g. ATTO647N or Cy3) are detected using a sensitive and rapid EM-CCD camera. Fluorescence excitation sources are CW lasers (e.g. frequency

doubled Nd:Yag laser, solid state laser or He:Ne laser). Excitation laser beams enter through the fluorescence epiport of the microscope and illuminate a wide field area of 10 to 20 μm in diameter of the sample by focusing the beam in the back aperture of the objective. For uPAINT, oblique illumination is required to avoid exciting the out of focus fluorescent ligands in the solution. This is achieved by translating the focused beam with respect to the axis of the objective, on the periphery of the back aperture of the objective (**Fig. 2**), akin to total internal fluorescence microscopy. Illumination intensities are of a few kW/cm^2 . For each type of dye used, an appropriate set of fluorescent filters is required. The total detection efficiency of a typical experimental single molecule setup is in the range of 5-10%.

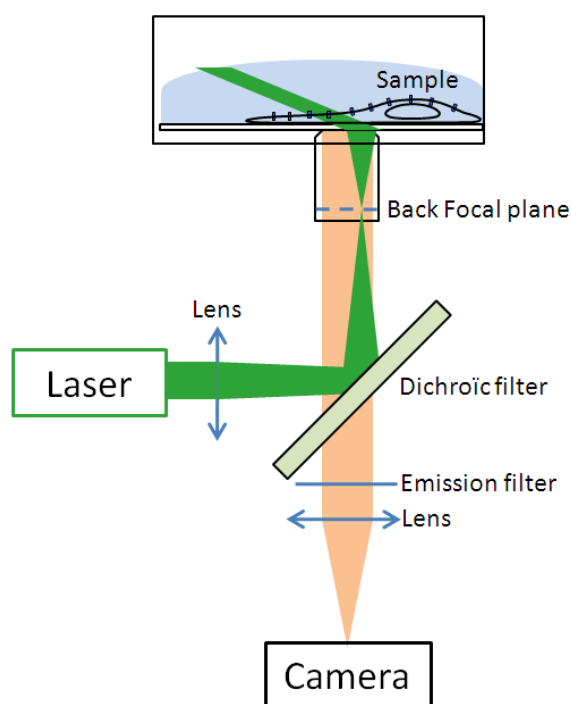


Figure 2: Schematics of the optical setup.

3.1.2 Resolution and trajectory lengths

With this detection efficiency, 1000 counts are commonly detected in 50 ms from a typical single fluorophore(11). This translates in a typical pointing accuracy (or localization precision) of 40-50 nm. We emphasize that different definitions of the pointing accuracy are often used. Here, we use the Full Width at Half Maximum (FWHM) of the distribution of the localizations obtained from a fixed molecule which is repetitively imaged. With this definition and using the Rayleigh criterion to define the resolution at which two molecules can be discriminated, the resolution is equal to the pointing accuracy. Some authors alternatively use the standard deviation of fixed molecule localizations for defining the pointing accuracy or localization precision, which provides values 2.3 times lower than

the definition used here. We generally prefer our definition, since, in the latter case, the pointing accuracy gives lower values than the resolution (factor of 2.3), which might induce confusing comparisons of different sets of data.

If longer integration times are used (at the price of fewer data points in a trajectory), improved pointing accuracies are obtained. For a shot noise limited detection, the pointing accuracy will improve with the inverse of the integration time (10) yielding $\sim 20\text{-}30$ nm resolution for 150 ms integration time. It is worth mentioning that when mobile molecules are imaged, the movement of the molecules might affect the pointing accuracy.

The number of points of a single molecule trajectory depends on the photo-physical properties of the imaged dye. In practice, and for a given dye, it depends on the excitation intensity and integration time used. Typically, one uses close to video rate imaging (50 ms integration times) at saturation intensities (~ 1 kW/cm² for the most common dyes). With these parameters, one can obtain typically 10-15 % of the trajectories lasting more than 1 s, in the case of ATTO647N dyes(7) (Figure 3).

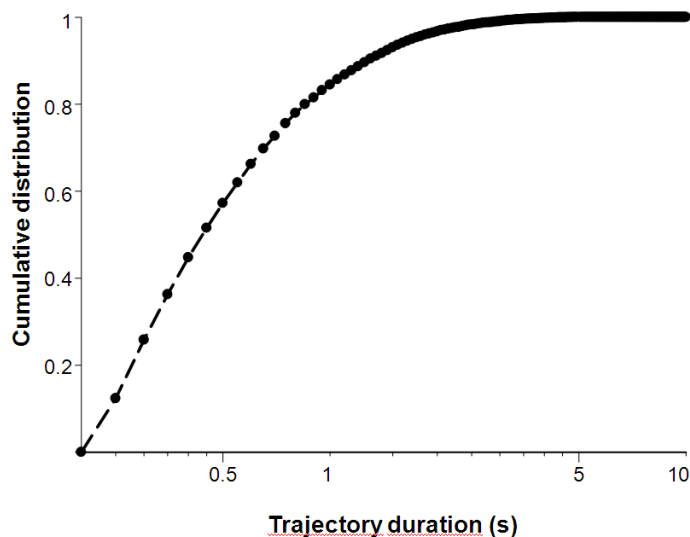


Figure 3: Distribution of single molecule trajectory lengths measured with ATTO647N on a live cell (adapted from (7)).

With uPAINT, and unlike standard single molecule methods, single point source emitter detection is ensured by the real time imaging of each individual ligand binding to its target membrane molecule regardless of the number of fluorophores it carries. Thus, one can take advantage of this feature to improve the pointing accuracy by coupling multiple dyes per ligand. For instance, with four fluorophores per ligand instead of one, the average pointing accuracy is improved by a factor of two under identical excitation intensity. Optionally, in order to lengthen the obtained trajectories, one can

reduce the excitation intensity while keeping the same pointing accuracy as when a single dye molecule is used(7).

3.1.3 Oblique illumination, choice of the angle.

By creating a thin sheet of light above the coverslip surface, oblique illumination allows selecting individual fluorescent ligands which have bound to the cell surface while rejecting the great majority of molecules in solution. This improves signal to noise ratios and avoids photobleaching of unbound fluorescent ligands. The choice of the angle depends on the thickness of the cells to be imaged. A typical choice is $\sim 5^\circ$ such that the resulting sheet of light has a thickness of $\Delta z \sim 2 \mu\text{m}$ in the center of the field of view. Assuming 3-dimensional isotropic diffusion of the fluorescent ligands freely diffusing in the solution, the diffusion coefficient D is well known and relates the ligand hydrodynamic diameter d and the fluid viscosity η by the Stokes-Einstein relation: $D = \frac{k_B T}{3\pi\eta d}$, where k_B is the Boltzmann constant and T is the temperature. For ligand hydrodynamic sizes of $d \sim 5\text{-}10 \text{ nm}$, D is of the order of $\sim 40\text{-}80 \mu\text{m}^2/\text{s}$ and the average time they spend in the 2D sheet of light is $2\Delta z^2/2D$ which lies below $\sim 100 \text{ ms}$. This indicates that such unbound fluorescent molecules should not appear statistically in more than one or two consecutive images if 50 ms integration times are used. Such unwanted events can be rejected in the analysis by omitting the first two molecular detections in each trajectory (see below).

3.2 Fluorescent labels

High affinity fluorescent ligands for the molecule to be studied are needed with uPAINT (*see Note 1*). We will describe here a procedure when an antibody is used as a label, either to study endogenous proteins when a high quality antibody is available or GFP expressed proteins using anti-GFP for instance. Other types of fluorescent labels can also be used depending on the proteins studied, such as Ni^{2+} tris-nitrilotriacetic acid (TrisNTA) when the target protein bears an extracellular poly-histidine tag(7, 12). The protocol for antibody labeling with ATTO647N-NHS-ester (Atto-Tech) is a modified version of the manufacturer's procedure. Keep in mind, that coupling a too low quantity of antibodies decreases the efficiency of the reaction. An amount of 200 to 300 μg is the minimum quantity required to obtain a good coupling.

1. For coupling, antibodies should be in an amine-free buffer. If the buffer contains amines, dialysis should be performed and antibodies should be resuspended in PBS 1X. For many commercial antibodies, addition of BSA is required during the experiments in order to decrease non-specific labeling. If this is the case, BSA should not be mixed to the antibodies during the antibody/dye labeling procedure to prevent preparing fluorescent BSA proteins.

2. Sodium carbonate (1M) should be added to the solution to obtain pH=8.3 necessary to protonate the amino group of lysines (about 100 μ L of NaHCO₃ per mL of antibody solution).
3. Fully dissolve 1 mg of ATTO647N-NHS-ester in 1mL of anhydrous, amine free DMSO. Then add a threefold molar excess of reactive dye to the antibody solution. Protect the sample from light and agitate for 3 hours at room temperature.
4. Use G-25 Sephadex columns to separate the conjugate from the free dye molecules. The columns are used with the gravity protocol. Equilibrate the column with PBS 1X. The first colored and fluorescent zone to elute will contain the conjugated antibodies. The second colored and fluorescent fraction contains the unlabeled free dye (hydrolyzed NHS-ester).
5. It is important to estimate the concentration of the different fractions and average number of dyes coupled per antibody. After coupling it is also crucial to test if the ATTO647N-NHS-ester binding does not affect the specificity of the antibody (this might happen if a lysine is present at the antibody binding site). In the latter case, ATTO647N-maleimide coupling can be a good alternative.

3.3 Sample preparation

Depending on the type of proteins and cells to be studied, the following example protocols may be modified. Although it is often more relevant to target endogenous proteins, in some cases the use of transfected proteins is required. In particular, this is the case when highly specific antibody against the protein of interest does not exist or for studies involving protein mutants. A convenient strategy is to fuse the protein of interest with an extracellular tag having known very good ligands (GFP, histidin tags, biotin/avidin, etc). Here, we describe two example protocols for studying exogenous or endogenous proteins (**Sections 3.3.1** and **3.3.2**, respectively). These protocols can be easily adapted to different kind of adherent cells (COS7, fibroblasts, etc) (*see Note 2*).

3.3.1. Exogenous proteins

This protocol gives the user tight control for reducing non-specific labeling on the surface of the coverslip which is a critical issue in uPAINT experiments.

1. Immortalized mouse embryonic fibroblasts and COS 7 cells are cultured in DMEM with 10% FBS.
2. Transient transfection of plasmids encoding membrane proteins fused to GFP or poly-histidine tags (GFP-GPI, 6His-Trans-Membrane) are performed using Fugene 6 .
3. The day of the experiment, cells are detached with trypsin/EDTA (0.05% for 2 min), trypsin inactivated with 10% FBS DMEM, washed and suspended in serum free condition in Ringer

medium, and incubated for 30 min before plating on the chosen extracellular matrix protein (rat collagen I or human fibronectin).

4. Experiments are performed 3 hours after cell plating. Optionally, cells can be co-transfected with a fluorescent protein reporting the sub-cellular localization of the region of interest (e.g. adhesion sites).

3.3.2. Endogenous proteins

Studying endogenous proteins depends on the availability of highly specific primary antibodies. Be aware that antibodies can affect the properties of the studied protein, promoting activation, inhibition, or cross-linking. Therefore, it is best to test in a functional assay if the antibody used for uPAINT affects the function of the target protein. In this example, endogenous AMPA receptors could be studied at the surface of live hippocampal neurons.

1. Cultures of hippocampal neurons are prepared from E18 Sprague-Dawley rats following the method previously described (13).
2. Cells are plated at a density of 200×10^3 cells/ml on poly-lysine pre-coated coverslips. To localize excitatory post-synapses, neurons can be electroporated (Lonza nucleofactor protocol) with Homer1C-GFP just after dissection and processed 2/3 weeks later.
3. Cultures are maintained in serum free neurobasal medium and kept at 37°C in 7.4% CO₂ for 10-15 days in vitro.

3.3.3. Preparing samples for imaging

1. Before acquisition, coverslips are incubated with a solution containing a low concentration of fluorescent beads. Adsorption of a few beads on the glass coverslip will provide immobile reference objects to correct long-term mechanical instabilities of the microscope. The concentration and incubation time should be adjusted so that 2 to 3 beads are present on average in the imaging field. Gentle rinsing is performed in order to avoid detaching adsorbed beads.
2. Then, a coverslip is mounted on an open chamber and 600 µl of recording medium is added onto the cells. This solution has to be free of vitamins and other cyclic compounds (present at high concentration in the culture medium) because of their intrinsic fluorescence which might produce unwanted background signals
3. Osmolarity has to be adjusted, by adding NaCl and/or glucose, depending on the osmolarity of the medium culture measured just before the experiment.
4. The acquisition is initiated when the area of the cell preparation to be studied is selected. Differential Interference Contrast or fluorescence imaging of a particular fluorescently tagged

protein can help to perform this selection (e.g. GFP imaging of excitatory synapses or other subcellular compartment). Once this selection is performed, the sample should not be moved throughout the experiment.

3.4 Acquisition

Images are typically acquired at video rates or faster, depending on the mobility of the investigated molecule. If the streaming mode of the camera is not used, a fast shutter synchronized with the camera can eventually be added in the excitation path to prevent sample illumination in between frames to limit dye photobleaching.

The acquisition procedure consists in recording several temporal stacks of images. For typical experiments, 3 to 4 stacks of 4000 images are recorded. Immediately after identification of the acquisition area and before the beginning of recording, 1-5 μL of fluorescent ligands are carefully added and the medium homogenized with 200 μl pipetman to avoid any mechanical drifts of the sample (**Fig. 4**).

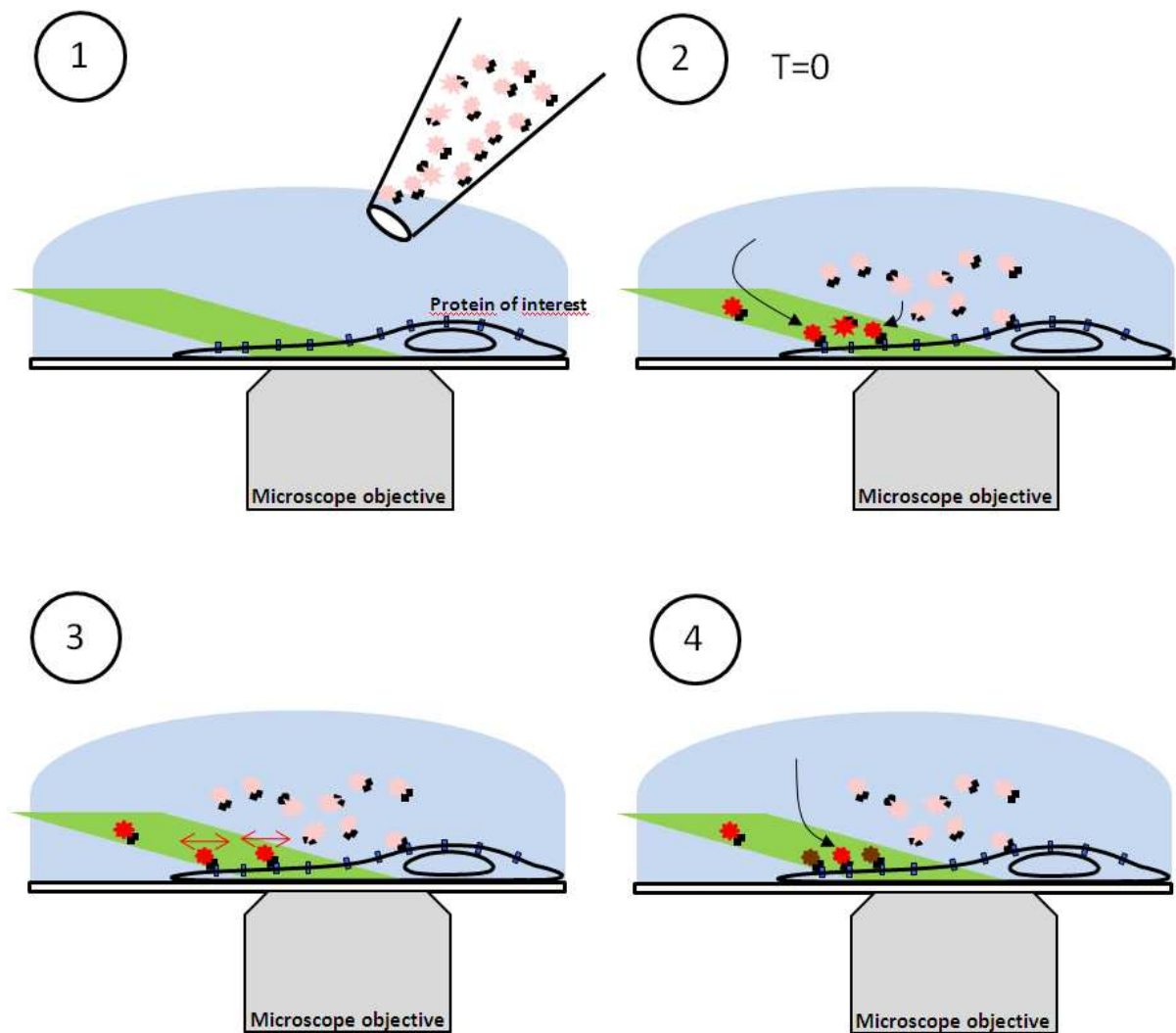


Figure 4: Cartoon of an imaging sequence. Non-illuminated dye molecules are displayed in pink, fluorescent ones in red and photobleached ones in brown.

Soon after the addition of the fluorescent ligands, diffraction limited fluorescent spots start to be visible in the field of view (**Fig. 5**). The quantity of ligands to be added has to be adjusted as a function of its affinity, and the desired labeling density (**Fig. 5**). For instance, the higher the protein mobility, the lower the spot spatial density should be in order to facilitate trajectory reconstructions and avoid trajectory mixing. To obtain super-resolved images with the highest resolutions, the highest signal to noise ratio should be obtained. This can be done by using the longest integration times compatible with molecule movements during each image but at the price of a loss of dynamic information due to fewer number of data points obtained in each trajectory. On the other hand, high content information on the dynamics of the molecules is better obtained at the highest imaging rates to obtain more data points per trajectories but at the price of slightly lower spatial resolutions. Thus, the

choice of the ligand concentration and imaging rates will result from a compromise and should be adjusted for each set of experiments.

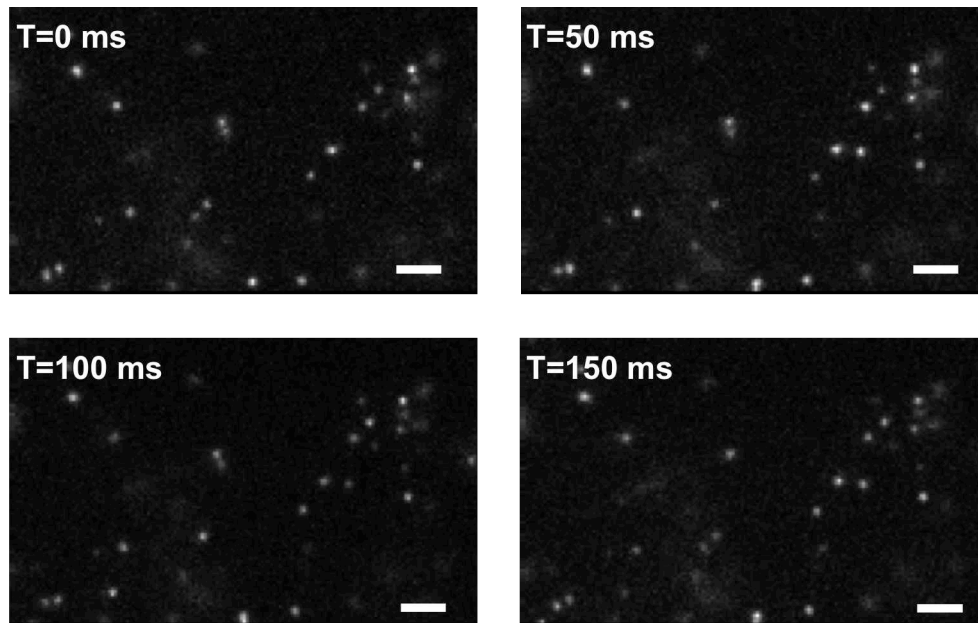


Figure 5: Typical raw images acquired at different times during the imaging sequence. Fluorescent spots appear stochastically at the surface of the living cell upon fluorescent ligand binding on their target. These spots can be tracked on several images as long as the fluorescent molecules do not photobleach. Scale bar: $5\mu\text{m}$.

It is also important to control the variation of the osmolarity during recording. For instance, in typical experiments at 37°C , where $600\ \mu\text{l}$ of mounted volume is used, the osmolarity increases by 20 mOsmol after 15 minutes of recording.

3.5 Analysis

This ultimate step allows quantifying and visualizing the localization and dynamics of the molecule of interest, at spatial resolution below the diffraction limit of light microscopy. We use custom made programs written in C/C++ and Visual Basic programming languages. These modules are launched as a DLL inside the Metamorph software environment in order to be able to visualize some preliminary results directly on the acquisition workstation.

3.5.1 Detection and trajectory analysis of single fluorescent ligand molecules

In each image of the recorded sequence, single fluorescent ligands appear as diffraction-limited bright spots. Two different approaches can be used, one based on centroid determination using wavelet transforms, and another one using Gaussian fitting.

Routine single dye localization can be performed using a wavelet transform segmentation process. We use the “à trous” algorithm with a B-Spline of third order (14), since it is very fast and provides very good pointing accuracy, similar to Gaussian fitting methods commonly used in super-resolution microscopy. We keep the second wavelet map, which contains most of the diffraction limited signal, while more than 80% of the noise is filtered in the first map and the background is contained in the larger maps. We then typically apply a fixed threshold of 1 to 2 times the background noise standard deviation. We use a custom watershed algorithm to separate close molecules. Finally, only the objects of surface superior to 3 pixels ($\sim 0.7 \mu\text{m}^2$) are kept. **Fig. 6b** displays a typical uPAINT image and the corresponding single molecule localization. A stack of dimension 128×128 pixels \times 5000 frames takes about 120 seconds to process on an Intel XEON 2.4GHz CPU, including the image loading to RAM, leading to about 50,000 detections and 3000 trajectories

As an alternative to wavelet transform analysis, the positions for each single molecule can be obtained by fitting the fluorescent signal by the following two-dimensional Gaussian function (11, 15, 16):

$$I(x, y) = I_0 \exp\left(-\frac{(x - x_0)^2 + (y - y_0)^2}{2\sigma^2}\right)$$

Where I_0 is the amplitude of the Gaussian (given as a grayscale value); σ is related to the FWHM of the diffraction pattern by $\text{FWHM} = 2.35\sigma$. Typically, the FWHM of the setup is around 350 nm for 660 nm emission wavelength. The parameters x_0 and y_0 give the central positions of the spot. The errors in the fitting coefficients vary for each analyzed spot because the fitting accuracy depends on the local signal-to-noise ratios. The FWHM of the distribution of x_0 and y_0 for fixed molecules represents the positioning accuracy (see definition and remarks above), which only depends on this signal-to-noise ratio and is typically well below the optical resolution limit of about 50 nm in this work.

Nevertheless, since the aim is to localize moving single molecules, the movement occurring during the image acquisition may affect the apparent shape of the signal. This prevents the Gaussian fitting with fixed calibrated size to be achieved accurately and motivates the use of segmentation based on centroid as the wavelet method presented above.

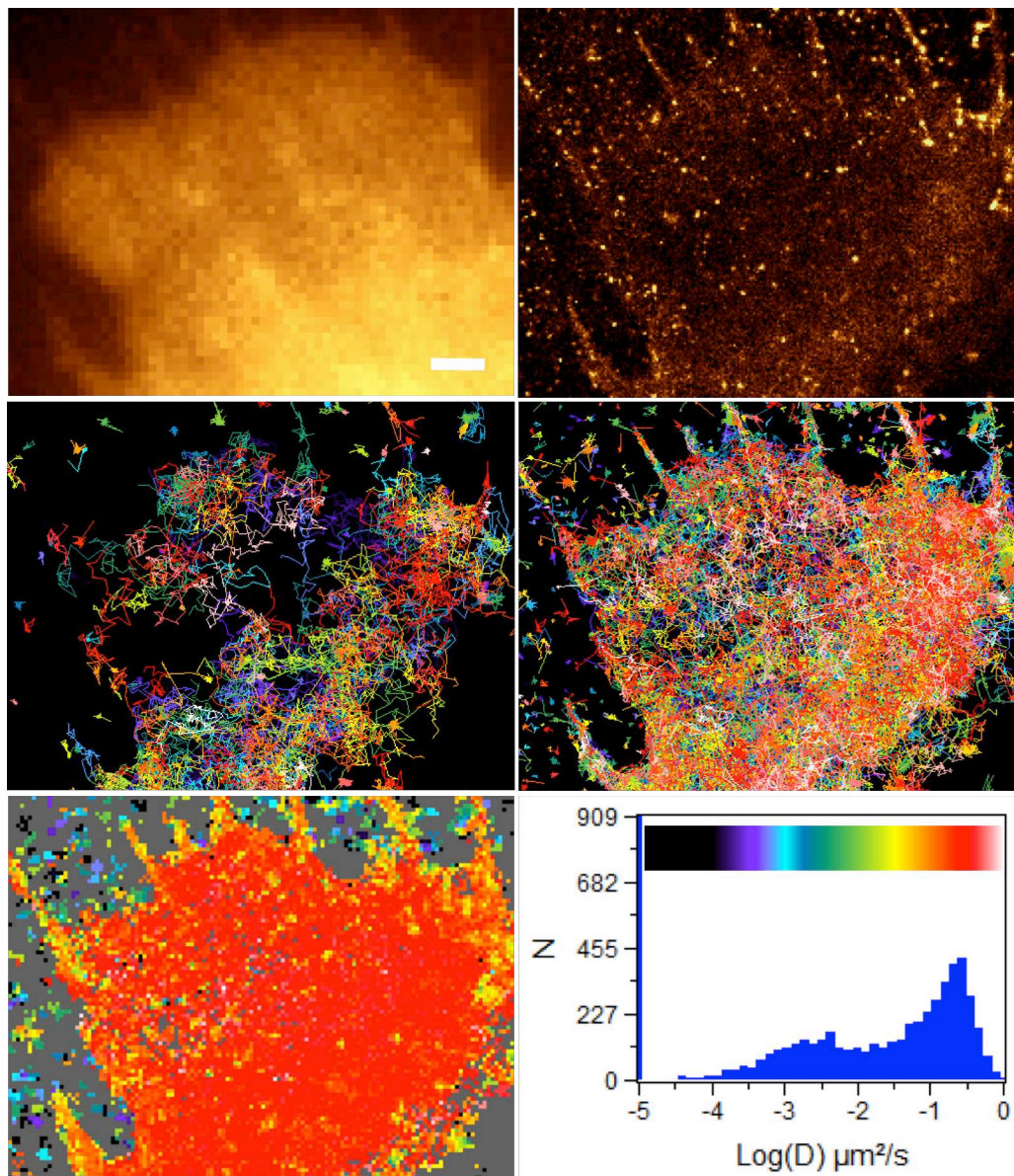


Figure 6: Illustration of the reconstruction. (a) Wide-field fluorescence image of a live fibroblast expressing cytosolic fluorescent GFP and a membrane protein of interest (here the transmembrane domain of the PDGF receptor(7)). Scale bar 1.5 μm . (b) super-resolved image reconstructed from 310000 localizations of fluorescent ligands (ATTO647N) which have bound to their target protein at the surface of the cell. Images of the protein trajectories with lengths > 50 points (c) and > 10 points (d) ($N=550$ resp. 6000). (e) diffusion map: spatially resolved color-coded diffusion constants of the proteins shown in (b-d) as defined in the histogram presented in (f) computed on trajectories with more than 20 points.

3.5.2 Trajectory reconstruction

Trajectories are reconstructed by connecting object positions from one image to the next. Several algorithms can be used. We use a global tracking method based on simulated annealing algorithm for

its flexibility and rapid convergence(17). It consists of minimizing a global energy function E , taking into account the intensity and velocity of each detected molecule. Since molecules are constantly appearing and disappearing in the field of view, “birth” and “death” events are also taken into account in the energy function. Only trajectories lasted more than several points (ten) are kept for further analysis. This allows the rejection of false single molecule detection that could occur due to noise, as well as, to keep trajectories which are long enough for quantification.

Low labeling densities are preferred to facilitate this process and minimize connection errors (see **Fig. 5** and **6**).

3.5.3 Super-resolved image reconstruction

Super-resolution images are reconstructed based on the numerous molecule localizations: all the molecules detected during the acquisition sequence are pooled to form a high-resolution image. Since the resolution of the super-resolved image depends on the localization accuracy of the single molecules, the user can define the pixel size of the super resolution image. The ideal sampling is defined as less than, or equal to, half of the resolution needed to satisfy the Nyquist criterion (18). Typically, a 256×256 image with a pixel size of 160 nm, analyzed with a resolution of 40 nm, will lead to a super-resolution image of dimension 2048×2048 with a pixel size of 20 nm (sub-sampling factor of 8 times). Each detected molecule will then contribute to the super-resolution image by adding a grey value at the localization coordinates.

It is possible to represent a super-resolution image of various additional parameters, like the intensities, trajectories, planes of detection, or any quantification performed on the mobility (see below). Thanks to high molecule density provided by uPAINT, it is also possible to perform the cartography of any of the quantification parameters by averaging all the measurements in pixels of dimensions defined by the user.

In order to take into account the possible drifts occurring during the total duration of the acquisition (which is in the range of few minutes), an automatic registration step is performed using the super localization and tracking of the immobile fluorescent beads recorded in the field of view. Tracks of the drift are computed and smoothed using a median filter of 5 before registration.

3.5.4 Dynamic quantification

Different types of dynamic information can be obtained from the analysis of the trajectories measured by uPAINT. We will list here a few standard ways of quantifying the molecules movements occurring on a cell, without aiming at being exhaustive about the analysis strategies.

For each trajectory, one can compute the mean square displacement (MSD), which measures the area covered by a molecule over time. For a trajectory of N data points (coordinates $x(t)$, $y(t)$ at times $t=0$ to $(N-1)*\Delta t$, with e.g. $\Delta t = 50$ ms, the inverse of the acquisition rate), the MSD for time intervals $\tau=n*\Delta t$ is calculated using the formulae:

$$MSD(n * \Delta t) = \sum_{i=1}^{N-n} \frac{[x((i+n) * \Delta t) - x(i * \Delta t)]^2 + [y((i+n) * \Delta t) - y(i * \Delta t)]^2}{N - n}$$

For the time interval $\tau=n \Delta t$, the MSD and its error bar are thus calculated on $N-n$ points.

The MSD is widely used to extract diffusion characteristics from trajectories. For instance, a linear MSD over time is characteristic of a molecule diffusing freely, while the confined movement of molecules in a domain is indicated by a plateau reached by its MSD over time. For each MSD, the instantaneous diffusion coefficient, D , can also be calculated from linear fits of the first 4 points (corresponding to 200 ms) of the MSD using $MSD(\tau) = \langle r^2 \rangle(\tau) = 4D\tau$. Histograms of the molecules diffusion constants measured on a large number of molecules on a given cell can thus be obtained (**Fig. 6f**).

Two-dimensional maps of molecule mobilities can also be produced by displaying in a color-coded pixel (whose size is chosen by the user, typically 200 nm) the median of the step lengths (corresponding to the distance between two consecutive points of a trajectory) found in this pixel(7) or the mean instantaneous diffusion constant of the molecules detected in this pixel (see **Fig. 6 e-f** for example). These types of maps provide dynamic information of subcellular regions of a given cell (7).

4. Notes

1. In uPAINT, the specificity of the ligand used is certainly the most crucial parameter. Indeed, on the contrary to other labeling procedures with external probes, one does not wash the preparation after placing the fluorescent ligand in solution. Thus, highly specific ligands should be used.
2. At the moment, this protocol is mainly dedicated to membrane protein imaging. The method can also be adapted to intracellular protein imaging in fixed permeabilized cells.

Acknowledgments

We wish to thank B. Lounis for helpful discussions. This research was funded by Centre National de la Recherche Scientifique (CNRS), the Région Aquitaine and the Agence Nationale pour la Recherche (ANR), the Fondation pour la Recherche Médicale and the European Union's seventh framework program for research and development ERC grant Nano-Dyn-Syn.

5. References

1. Hell, S.W. (2007) Far-Field Optical Nanoscopy. *Science* **316**, 1153-1158.
2. Huang, B., Bates, M., and Zhuang X. (2009) Super-Resolution Fluorescence Microscopy. *Annual Review of Biochemistry* **78**, 993-1016.
3. Betzig, E., *et al.* (2006) Imaging Intracellular Fluorescent Proteins at Nanometer Resolution. *Science* **313**, 1642-1645.
4. Hess, S.T., Girirajan, T.P., and Mason, M.D. (2006) Ultra-high resolution imaging by fluorescence photoactivation localization microscopy. *Biophys J* **91**, 4258-4272.
5. Rust, M.J., Bates, M., and Zhuang, X.W. (2006) Sub-diffraction-limit imaging by stochastic optical reconstruction microscopy (STORM). *Nature Methods* **3**, 793-795.
6. Geissbuehler, S., Dellagiacoma, C., and Lasser, T. (2011) Comparison between SOFI and STORM. *Biomed. Opt. Express* **2**, 408-420.
7. Giannone G, *et al.* (2010) Dynamic Superresolution Imaging of Endogenous Proteins on Living Cells at Ultra-High Density. *Biophys J* **99**, 1303-1310.
8. Sharonov, A. and Hochstrasser, R.M. (2006) Wide-field subdiffraction imaging by accumulated binding of diffusing probes. *PNAS* **103**, 18911-18916.
9. Bobroff, N. (1986) Position measurements with a resolution and noise-limited instrument. *Review of Scientific Instruments* **57**, 1152-1157.
10. Thompson, R.E., Larson, D.R., and Webb, W.W. (2002) Precise Nanometer Localization Analysis for Individual Fluorescent Probes. *Biophys. J.* **82**, 2775-2783.
11. Tardin, C., Cognet, L., Bats, C., Lounis, B., and Choquet, D. (2003) Direct imaging of lateral movements of AMPA receptors inside synapses. *EMBO J.* **22**, 4656-4665.
12. Grunwald C, *et al.* (2011) Quantum-Yield-Optimized Fluorophores for Site-Specific Labeling and Super-Resolution Imaging. *Journal of the American Chemical Society* **133**, 8090-8093.
13. Groc L, *et al.* (2004) Differential activity-dependent regulation of the lateral mobilities of AMPA and NMDA receptors. *Nat Neurosci.* **7**, 695-696.
14. Starck, J-L. and Murtagh, F. (2006) *Astronomical Data and Image Analysis* (Springer) 2nd edition Ed.
15. Schmidt, T., Schuetz, G.J., Baumgartner, W., Gruber, H.J., and Schindler, H. (1996) Imaging of single molecule diffusion. *Proc.Natl.Acad.Sci.U.S.A.* **93**, 2926-2929.
16. Cheezum, M.K., Walker, W.F., and Guilford, W.H. (2001) Quantitative Comparison of Algorithms for Tracking Single Fluorescent Particles. *Biophys. J.* **81**, 2378-2388.
17. Racine, V., *et al.* (2006) Multiple-target tracking of 3D fluorescent objects based on simulated annealing. *2006 3rd IEEE International Symposium on Biomedical Imaging: Macro to Nano, Vols 1-3*, IEEE International Symposium on Biomedical Imaging, pp 1020-1023.
18. Shannon, C.E. (1949) Communication in the Presence of Noise. *Proceedings of the IRE* **37**, 10-21.